ISSN: 2771-7887

Research Article

New Advances in Brain & Critical Care

Hippocampal Ripples are Correlated with Subthreshold Up/Down Activity in Mouse Posterior Parietal Cortical Neurons

Hiroyuki Mizuno[1] and Yuji Ikegaya[1,2,3*]

[1]*Graduate School of Pharmaceutical Sciences, The University of Tokyo, Japan*

[2]*Institute of AI and Beyond, The University of Tokyo, Japan*

[3]*Center for Information and Neural Networks, National Institute of Information and Communications Technology, Japan*

[*]Corresponding Author
Yuji Ikegaya, Graduate School of Pharmaceutical Sciences, Institute of AI and Beyond and Center for Information and Neural Networks, National Institute of Information and Communications Technology, The University of Tokyo, Japan.

Submitted: 2024, May 04; **Accepted:** 2024, May 24; **Published:** 2024, May 31

Citation: Mizuno, H., Ikegaya, Y. (2024). Hippocampal Ripples are Correlated with Subthreshold Up/Down Activity in Mouse Posterior Parietal Cortical Neurons. *New Adv Brain & Critical Care, 5*(1), 01-07.

Abstract

Memories acquired during wakefulness are consolidated during sleep. During non-rapid eye movement (NREM) sleep, ripples occur in the hippocampus, while slow oscillations (SOs) occur in the neocortex. The coupling of ripples and SOs is believed to play a key role in memory consolidation. The posterior parietal cortex (PPC) is one of the regions that exhibit reactivation around the occurrence of ripples. Recent studies have revealed subthreshold membrane potential dynamics of PPC neurons after ripples. However, it remains unclear whether these membrane potential dynamics depend on the timing of ripples relative to the phase of SOs. We performed whole-cell recordings from neurons in the PPC and simultaneous LFP recordings from hippocampal CA1. Membrane potentials during SOs were classified into UP and DOWN states, and ripples were detected from the LFP recording. Analyses of the timing of ripples relative to the phases of SOs revealed that they preferentially occurred near the transition between UP and DOWN states. The timing of the ripples relative to the transitions was correlated with the duration and amplitude of the UP and DOWN states. Therefore, the phase of SOs may modulate the effects of ripples on the neocortex.

Keywords: Whole-Cell Recording, Hippocampal Ripples, Slow Waves, Posterior Parietal Cortex

1. Introduction

Memories formed during wakefulness are consolidated during sleep, a process thought to rely on communication between the neocortex and the hippocampus [1,2]. During non-rapid eye movement (NREM) sleep or under anaesthesia, neocortical activity is characterized by slow oscillations (SOs), whereas hippocampal activity is characterized by ripples. SOs are sustained oscillations at low frequencies (0.5-4 Hz) that alternate between active (UP) and inactive (DOWN) states [3,4]. Hippocampal ripples, on the other hand, are transient high-frequency waves (100-250 Hz) that play a key role in memory consolidation [5,6].

Previous research has emphasized the importance of coordination between ripples and SOs for memory consolidation [2,7,8]. Investigations of this coordination have primarily focused on the temporal coupling between these two waves. Ripples tend to occur more frequently during UP states than DOWN states, with their event rate peaking around transitions between UP and DOWN states [7,9].

In addition, population activity studies have shown that several neocortical regions show reactivation around ripples. The posterior parietal cortex (PPC) is one of the regions whose reactivation correlates with the occurrence of ripples [10]. Recent efforts using whole-cell recording have further revealed subthreshold activity patterns of neocortical neurons, revealing the existence of depolarized and hyperpolarized neurons around ripples [11-13]. However, the impact of ripple timings relative to the SO phases on subthreshold membrane potentials (*V*ms) remains unclear.

To address this knowledge gap, we conducted whole-cell patch clamp recordings from neurons in the PPC simultaneously with local field potential (LFP) recordings from hippocampal CA1 of mice under anaesthesia. We categorized *V*m traces into UP and DOWN states and identified ripples from LFP recordings. We found that the timings of ripples correlated with subthreshold *V*m dynamics of the PPC neurons. This result suggests that ripples at a specific timing relative to the phase of SOs affect neocortical neuronal activity.

2. Methods

2.1. Animals

Animal experiments were performed under the approval of the Animal Experimentation Ethics Committee of the University of Tokyo (approval number: P4-2) and in accordance with the Guidelines for the Care and Use of Laboratory Animals of the University of Tokyo. These experimental protocols were conducted in accordance with the Basic Guidelines for the Proper Conduct of Animal Experiments and Related Activities in Academic Research Institutions (Ministry of Education, Culture, Sports, Science and Technology, Notice No. 71 of 2006), the Standards for Breeding and Housing of and Pain Relief for Laboratory Animals (Ministry of the Environment, Notice No. 88 of 2006), and the Guidelines for the Method of Animal Disposal (Prime Minister's Office, Notice No. 40 of 1995). All animals were housed under a 12-h dark/light cycle (light from 07:00 to 19:00) at 22 ± 1°C with ad libitum food and water.

2.2. Surgery

Male ICR mice aged 28-40 days were anesthetized with urethane (2.25 g/kg, i.p.) as previously described [13]. Anaesthesia was confirmed by the absence of paw withdrawal, whisker movement, and eyeblink reflexes. The skin was removed from the head and a metal head plate was attached to the skull. A craniotomy (2.5 × 2.0 mm2) was performed above the right hemisphere centred 2.0 mm posterior to bregma and 2.5 mm ventrolateral to the sagittal suture, and the dura was surgically removed. The exposed cortical window was covered with 1.7 % agar at a thickness of 1.5 mm.

2.3. Electrophysiology

LFPs were recorded from the hippocampal CA1 stratum pyramidale by using a tungsten electrode (3.5–4.5 MΩ, catalog #UEWMGCSEKNNM, FHC, USA) coated with a crystalline powder of 1,1'-dioctadecyl-3,3,3',3'-tetramethylindocarbocyanine perchlorate (DiI). The location of the recording site was confirmed by the occurrence of ripples. Whole-cell recordings were obtained from layer 2/3 neurons in the PPC (AP: 1.2-3.5 mm posterior to bregma; ML: 0.60-2.51 mm from the sagittal suture; DV: 40-520 µm ventral to the dura) using borosilicate glass electrodes (3.9-7.1 MΩ). Liquid junction potentials were automatically corrected before each experiment using the Pipette Offset mode (Molecular Devices) and were not corrected post hoc. Principal cells were identified based on their regular spiking properties and by post hoc histological analysis. The intrapipette solution consisted of the following reagents: 135 mM K-gluconate, 4 mM KCl, 10 mM HEPES, 10 mM creatine phosphate, 4 mM MgATP, 0.3 mM Na_2GTP, 0.3 mM EGTA (pH 7.3), and 0.2% biocytin. At the beginning of each experiment, we injected 1-s square currents of -200–200 pA into the cell in 50-pA ascending steps to examine whether it was a putative excitatory or inhibitory neuron based on its spike responses. In general, excitatory and inhibitory neurons exhibit regular-spiking and fast-spiking firing patterns, respectively [14]. Regular-spiking neurons were selected for the subsequent analyses. Cells were discarded when the mean resting potentials exceeded -55 mV or when the action potentials were below -20 mV. Signals recorded with tungsten electrodes and glass electrodes were amplified using a DAM80 AC differential amplifier and a MultiClamp 700B amplifier, respectively. Both types of signals were digitized at a sampling rate of 20 kHz using a Digidata 1322A or 1550B digitizer that was controlled by pCLAMP 10.7 software (Molecular Devices).

2.4. Histology

Following each experiment, the electrodes were carefully removed from the brain. To visualize the patch-clamped neurons, the mice were transcardially perfused with 4% paraformaldehyde, and the brains were fixed in 4% paraformaldehyde overnight at room temperature. We then recovered the morphology of the recorded neurons by the following methods. Brains were sliced sagittally at 100 µm thickness using a vibratome. Sections were incubated with 2 µg/ml streptavidin-Alexa Fluor 594 conjugate and 0.1% Triton X-100 for 4 h, followed by incubation with 0.4% NeuroTrace 435/455 (N21479, Thermo Fisher Scientific, Waltham, MA, USA) and 0.3% Triton X-100 for 1.5 h. Fluorescence images were acquired using a confocal microscope (FV1200, Olympus, Tokyo, Japan).

2.5. Definition of UP/DOWN State from Membrane Potentials

The MAUDS method, Seamari et al, was used to classify the *V*ms into UP (depolarizing) and DOWN (hyperpolarizing) states [15]. *V*ms recorded at 20 kHz sampling rate were downsampled to 2 kHz and used, and two different moving average filters were applied to the *V*ms. One moving average filter was applied with a width of 6 s and the other with a width of 0.05 s. The former was defined as V_{slow} and the latter was defined as V_{fast}. The period when $V_{fast} > V_{slow}$ was defined as the UP state and the period when $V_{fast} < V_{slow}$ was defined as the DOWN state. However, UP/DOWN states with durations of 0.04 s or less were eliminated.

2.6. Hippocampal Ripple Detection

To detect hippocampal ripple events, hippocampal LFP traces were downsampled to 2 kHz and were band-pass filtered at 100-250 Hz, and the root-mean-square (RMS) power was calculated in the band with a bin size of 5 ms. The threshold for ripple detection was set to 3 × standard deviations (SDs) above the mean. Ripple onsets and offsets were marked at the points where the ripple power first exceeded or fell below 3 × SDs above the mean, and events lasting < 15 ms were excluded.

2.7. Classification of Ripple State and Non-Ripple States

We discriminated between ripple and non-ripple states using kernel density estimation applied to the detected ripples. The estimated densities were z-scored, and periods where this exceeded -0.5 were defined as ripple states, while the rest were defined as non-ripple states. However, ripple states shorter than 20 seconds and non-ripple states shorter than 10 seconds were excluded.

2.8. Statistical Analysis

Data were analysed offline using custom-made MATLAB (R2022a and R2024a, Natick, Massachusetts, USA) routines. In Figure 3. to investigate the relationship between the timing of

ripples relative to UDt or DUt and *V*m fluctuations, we created shuffled data by shuffling the timing of ripples. The timings of ripples within the same ripple state were shuffled without altering their relative timings. We generated 10,000 sets of shuffled data. The grey backgrounds in Figure 3 represent the 99% confidence intervals, and data points outside this range were defined as statistically significant.

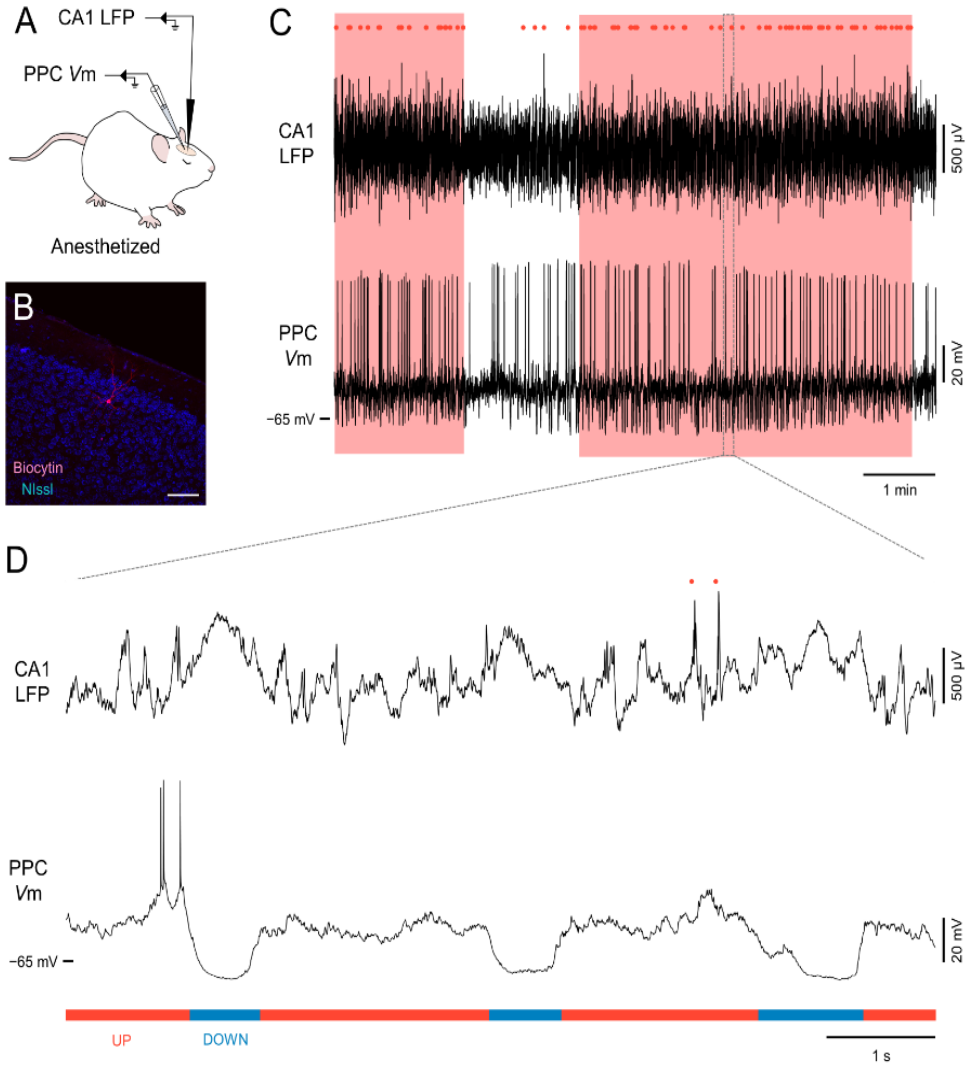

Figure 1: Simultaneous recording of CA1 LFPs and PPC neuronal Vms. (A) Schematic of simultaneous recording of hippocampal CA1 LFPs and PPC neuron Vms. (B) A representative fluorescence image of the recorded neuron (scale bar = 100 μm). (C) Representative traces of CA1 LFPs and Vms of PPC neurons. The red dots at the top of the figure indicate the onset of hippocampal ripples, and the red backgrounds represent the ripple state. (D) The magnified traces within the square frame outlined with a grey dotted line from (C)

3. Results

We performed whole-cell recording of PPC neurons simultaneously with extracellular recording of LFPs from hippocampal CA1 stratum pyramidale of mice under urethane anaesthesia, as a model of NREM sleep, to investigate the subthreshold *V*m dynamics of PPC neurons around hippocampal ripples (Figure 1A) [16,17]. Biocytin was added to the intrapipette solution for whole-cell recording, and recorded neurons were fluorescently stained post hoc (Figure 1B). The LFP recording site was confirmed by the occurrence of ripples characteristic of hippocampal CA1. A previous study revealed that the neocortex and hippocampus alternate between NREM sleep-like states and REM sleep-like states when mice are anesthetized with urethane [17]. Hippocampal ripples are more likely to occur during NREM sleep [18]. Biases in the occurrence of hippocampal ripples were also observed in our data. We classified the recorded traces into the state with more hippocampal ripples (ripple state) and the state with fewer hippocampal ripples (non-ripple state), and we used LFP and *V*m data during ripple states for subsequent analyses (Figure 1C). *V*ms during ripple states exhibited bistable dynamics and were not observed during non-ripple states. This result suggests that ripple states are consistent with NREM sleep-like states. Therefore, we separated the *V*m traces into UP/DOWN states (Figure 1D).

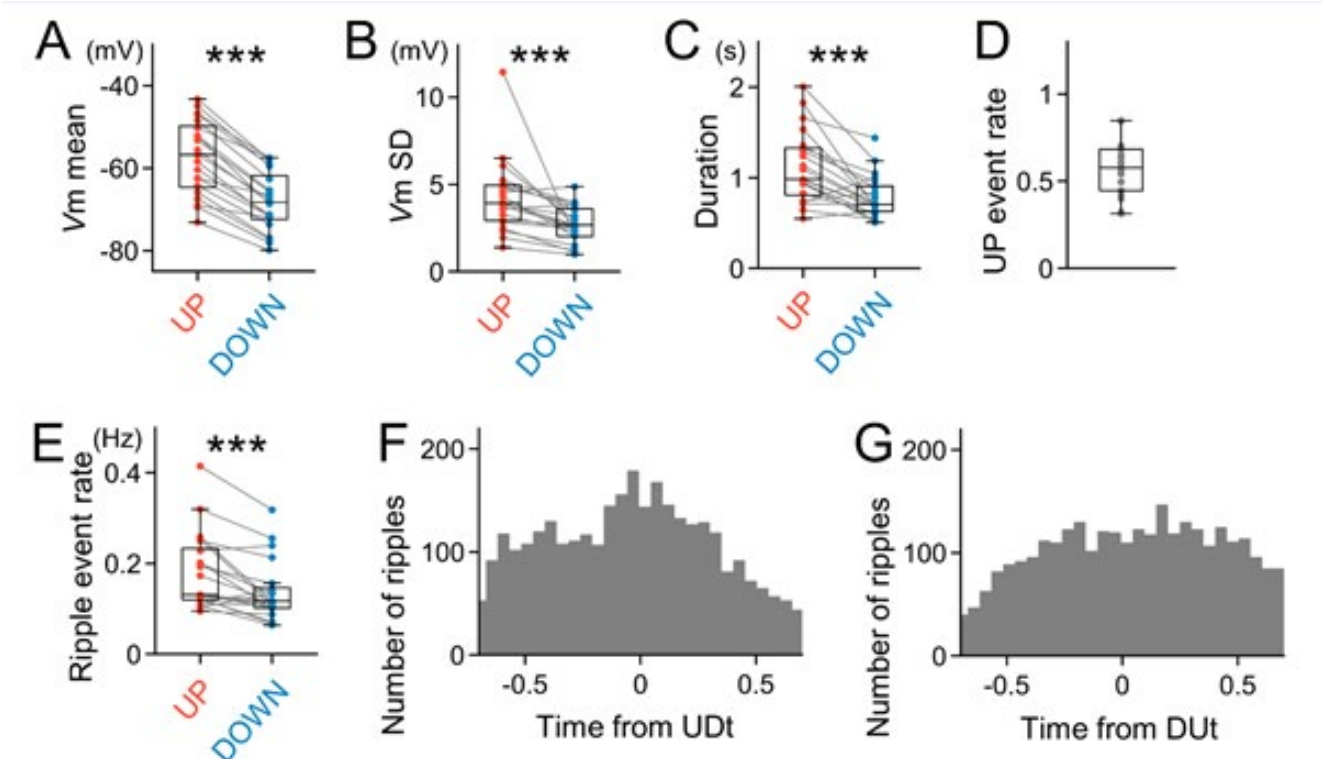

Figure 2: Hippocampal ripples occur preferentially at a specific phase of SOs. (A-C) Comparison of Vm parameters between UP and DOWN states. mean Vm (A), SD of Vm (B) and duration (C) were compared ($^{***}P < 0.001$). (D) Event rate of UP states. (E) Comparison of hippocampal ripple event rates between UP and DOWN states ($^{***}P< 0.001$). (F) Histogram of ripple occurrence around UP to DOWN transitions (UDt). (G) Histogram of ripple occurrence around DOWN to UP transitions (DUt).

First, we compared *V*ms during UP and DOWN states. The mean *V*m, standard deviation (SD) of *V*m and duration were significantly different between UP and DOWN states (Figure 2A-C, *V*m mean: UP = -57.3 ± 8.9 mV, DOWN = -68.0 ± 7.1 mV, $Z = 4.0$, $P = 6.0\times10^{-5}$; SD of *V*m: UP = 4.2 ± 2.1 mV, DOWN = 2.7 ± 1.0 mV, $Z = 3.9$, $P = 1.0\times10^{-4}$; Duration: UP = 1.12 ± 0.39 s, DOWN = 0.78 ± 0.23 s, $Z = 3.6$, $P = 3.7\times10^{-4}$, $n = 21$ cells from 18 mice, respectively, Wilcoxon signed-rank sum test). The mean of the UP-state event rate was 0.57 ± 0.15 Hz, which corresponds to a frequency of SOs (Figure 2D, $n = 21$ cells from 18 mice). We also calculated the hippocampal ripple event rate during the UP and DOWN states. Consistent with previous studies, the hippocampal ripple event rate was higher during UP states than during DOWN states (Figure 2E, UP = 0.180 ± 0.083 Hz, DOWN = 0.137 ± 0.066 Hz, $Z = 3.3$, $P = 9.0\times10^{-4}$, $n =$ 21 cells from 18 mice, respectively, Wilcoxon signed-rank sum test). Some research revealed that hippocampal ripples are more likely to occur around the transitions between UP and DOWN states. Our analyses suggest that the ripple event rate was high around the UP to DOWN transition (Figure 2F and 2G, $n = 21$ cells from 18 mice).

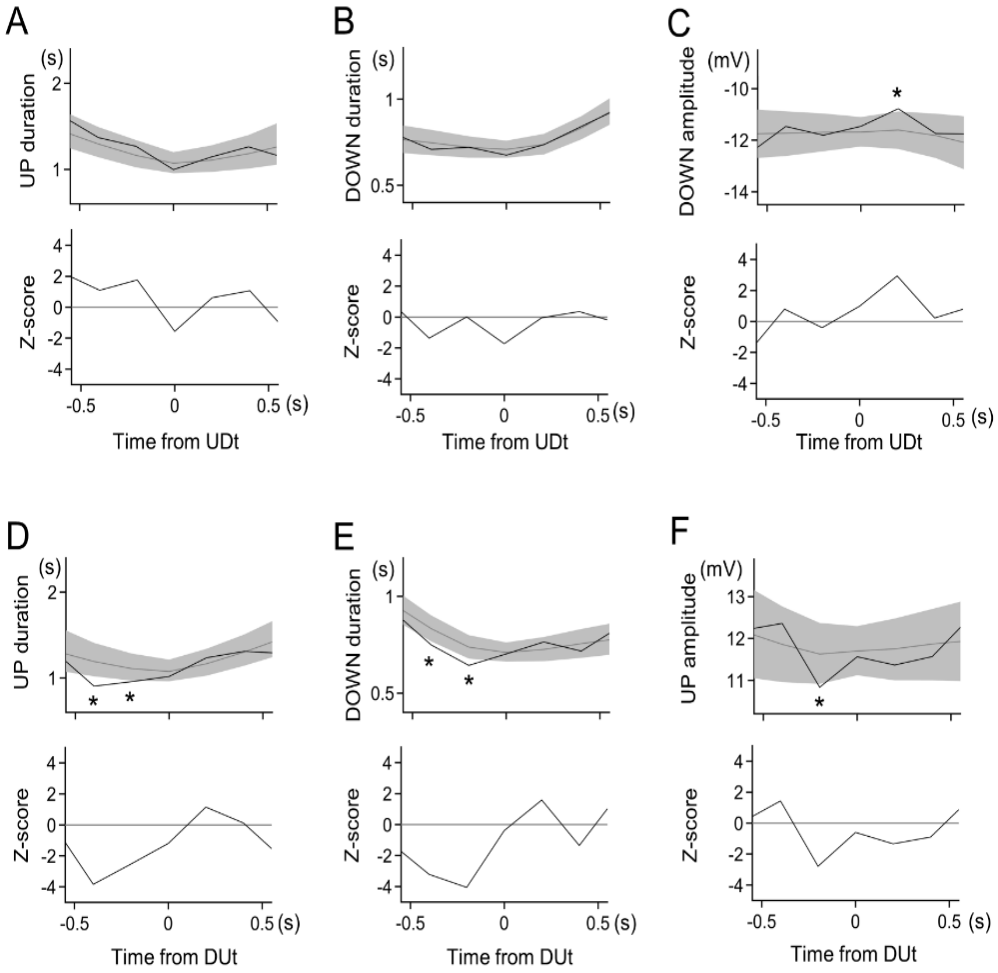

Figure 3: Hippocampal ripples differentially affect the Vms of PPC neurons depending on the SO phase. (A-C) The relationship between the timing of ripples relative to the UP-to-Down transition (UDt) and UP duration before UDt (A), DOWN duration after UDt (B), and DOWN amplitude after UDt (C). (D-E) The relationship between ripple timing relative to the DOWN-to-UP transition (DUt) and UP duration after DUt (D), DOWN duration before DUt (E), and UP amplitude after DUt (F). Gray areas indicate 99% confidence intervals. Asterisks (*) indicate that real data were outside the 99% confidence intervals.

To evaluate how ripples correlate with *V*m of neocortical neurons, we examined the timing of hippocampal ripples relative to the phases of SOs and *V*m dynamics by comparing the real and shuffled data. At the UP-to-DOWN transition, mean *V*ms during DOWN states were significantly high when hippocampal ripples occurred near the transitions (Figure 3 A-C). On the other hand, at the DOWN-to-UP transition, the durations of UP and DOWN states were significantly long, and mean *V*ms during UP states were significantly low when hippocampal ripples occurred near the transitions (Figure 3 D-F).

4. Discussion

We conducted simultaneous whole-cell recordings from neurons in the PPC and LFP recordings from the hippocampal CA1 region in urethane-anesthetized mice. We categorized recorded *V*ms into UP and DOWN states and identified hippocampal ripples from the LFP signals. Our analysis revealed a bias in the timing of hippocampal ripples relative to the phase of slow oscillations (SOs). Additionally, the timing of ripples around UP/DOWN transitions correlated with the duration of these states and *V*m fluctuations. These findings suggest that the impact of hippocampal ripples on neocortical neurons is dependent on the phase of SOs.

Previous studies have shown that activities across wide brain regions are modulated during hippocampal ripples, as observed through wide-field optical imaging or extracellular unit recordings with multi-channel electrodes [19-21]. Recent research employing simultaneous recordings of neocortical neuronal *V*ms and hippocampal CA1 LFPs has investigated subthreshold *V*m fluctuations following hippocampal ripple events [11-13]. These studies have indicated that neurons can be regulated in both depolarization and hyperpolarization directions by hippocampal ripples. However, it remains unclear whether these fluctuations in *V*m correlate with the phase of SOs. SOs are not solely generated by interactions between the neocortex and thalamus but are also believed to be influenced by hippocampal activities [22,23]. Given that a specific region may influence both neocortical and hippocampal activities, accurately evaluating the effect of hippocampal ripples on neocortical neurons becomes

challenging [22,24]. In this study, we analysed *V*m dynamics during UP-DOWN or DOWN-UP transitions and compared them with shuffled data to control for the effects of neocortical slow oscillations. Our results suggest that the response of PPC neurons to hippocampal ripples depends on the phases of SOs.

While it has been suggested that PPC neurons are influenced by hippocampal ripples, direct anatomical connections between the PPC and hippocampal CA1 are lacking [10,13]. The retrosplenial cortex (RSC) emerges as a candidate region for relaying activity, as it is connected to both the PPC and the hippocampus [25]. The RSC receives direct inputs from the subiculum, a region responsible for outputs from the hippocampal formation [26,27]. Recent studies examining RSC activity around hippocampal ripples have proposed that RSC neurons are suppressed following hippocampal ripple events [11,28]. Previous analyses suggested that UP-to-DOWN transitions are induced by hippocampal ripples [23,28]. These findings are consistent with our observation that hippocampal ripples are more likely to occur during UP-to-DOWN transitions. Our results suggest that following the occurrence of ripples during transitions from UP-to-DOWN states, the subsequent DOWN state becomes more depolarized. This implies that while ripples may suppress activity throughout the neocortex, they may selectively activate a subset of cells during DOWN states [29]. Conversely, when ripples occur during transitions from DOWN to UP states, the subsequent UP state becomes more hyperpolarized, suggesting that ripples may selectively target cells for inhibition during UP states. This phenomenon may underlie the coordinated reactivation between the hippocampus and neocortex [30].

5. Conclusions

This study elucidates the modulation of neocortical neuronal activity by hippocampal ripples as a function of the phase of neocortical slow oscillations (SOs). We found that hippocampal ripples occurring during UP/DOWN transitions exhibit frequency and potency in influencing neocortical neuronal membrane potentials. Understanding the dynamic interaction between the hippocampus and neocortex provides insight into the mechanisms of memory consolidation, but the causal relationship between ripple timing and memory consolidation remains unclear. Future studies should investigate whether optogenetic stimulation of hippocampal neurons at specific SO phases during sleep affects task performance.

Acknowledgments

This work was supported by JST ERATO (JPMJER1801), JSPS Grants-in-Aid for Scientific Research (22K21353), AMED CREST (22gm1510002h0002), and the Institute for AI and Beyond of the University of Tokyo.

References

1. Mölle, M., Yeshenko, O., Marshall, L., Sara, S. J., & Born, J. (2006). Hippocampal sharp wave-ripples linked to slow oscillations in rat slow-wave sleep. *Journal of neurophysiology, 96*(1), 62-70.
2. Sirota, A., Csicsvari, J., Buhl, D., & Buzsáki, G. (2003). Communication between neocortex and hippocampus during sleep in rodents. *Proceedings of the National Academy of Sciences, 100*(4), 2065-2069.
3. Chauvette, S., Crochet, S., Volgushev, M., & Timofeev, I. (2011). Properties of slow oscillation during slow-wave sleep and anesthesia in cats. *Journal of Neuroscience, 31*(42), 14998-15008.
4. Steriade, M., Nunez, A., & Amzica, F. (1993). A novel slow (< 1 Hz) oscillation of neocortical neurons in vivo: depolarizing and hyperpolarizing components. *Journal of neuroscience, 13*(8), 3252-3265.
5. Buzsáki, G., Horvath, Z., Urioste, R., Hetke, J., & Wise, K. (1992). High-frequency network oscillation in the hippocampus. *Science, 256*(5059), 1025-1027.
6. Girardeau, G., Benchenane, K., Wiener, S. I., Buzsáki, G., & Zugaro, M. B. (2009). Selective suppression of hippocampal ripples impairs spatial memory. *Nature neuroscience, 12*(10), 1222-1223.
7. Maingret, N., Girardeau, G., Todorova, R., Goutierre, M., & Zugaro, M. (2016). Hippocampo-cortical coupling mediates memory consolidation during sleep. *Nature neuroscience, 19*(7), 959-964.
8. Siapas, A. G., & Wilson, M. A. (1998). Coordinated interactions between hippocampal ripples and cortical spindles during slow-wave sleep. *Neuron, 21*(5), 1123-1128.
9. Isomura, Y., Sirota, A., Özen, S., Montgomery, S., Mizuseki, K., Henze, D. A., & Buzsáki, G. (2006). Integration and segregation of activity in entorhinal-hippocampal subregions by neocortical slow oscillations. *Neuron, 52*(5), 871-882.
10. Wilber, A. A., Skelin, I., Wu, W., & McNaughton, B. L. (2017). Laminar organization of encoding and memory reactivation in the parietal cortex. *Neuron, 95*(6), 1406-1419.
11. Chambers, A. R., Berge, C. N., & Vervaeke, K. (2022). Cell-type-specific silence in thalamocortical circuits precedes hippocampal sharp-wave ripples. *Cell reports, 40*(4), 111132.
12. Samejima, H., Sato, Y., & Ikegaya, Y. (2023). Visual Cortical Neurons Depolarize after Hippocampal Ripples. *New Advances in Brain & Critical Care, 4*(1), 1-5.
13. Sato, Y., Mizuno, H., Matsumoto, N., & Ikegaya, Y. (2021). Subthreshold membrane potential dynamics of posterior parietal cortical neurons coupled with hippocampal ripples. *Physiology International, 108*(1), 54-65.
14. McCormick, D. A., Connors, B. W., Lighthall, J. W., & Prince, D. A. (1985). Comparative electrophysiology of pyramidal and sparsely spiny stellate neurons of the neocortex. *Journal of neurophysiology, 54*(4), 782-806.
15. Seamari, Y., Narváez, J. A., Vico, F. J., Lobo, D., & Sanchez-Vives, M. V. (2007). Robust off-and online separation of intracellularly recorded up and down cortical states. *PloS one, 2*(9), e888.
16. Clement, E. A., Richard, A., Thwaites, M., Ailon, J., Peters, S., & Dickson, C. T. (2008). Cyclic and sleep-like spontaneous alternations of brain state under urethane anaesthesia. *PloS one, 3*(4), e2004.
17. Pagliardini, S., Gosgnach, S., & Dickson, C. T. (2013). Spontaneous sleep-like brain state alternations and breathing

characteristics in urethane anesthetized mice. *PLoS One, 8*(7), e70411.
18. Headley, D. B., Kanta, V., & Paré, D. (2017). Intra-and interregional cortical interactions related to sharp-wave ripples and dentate spikes. *Journal of neurophysiology, 117*(2), 556-565.
19. Karimi Abadchi, J., Nazari-Ahangarkolaee, M., Gattas, S., Bermudez-Contreras, E., Luczak, A., McNaughton, B. L., & Mohajerani, M. H. (2020). Spatiotemporal patterns of neocortical activity around hippocampal sharp-wave ripples. *elife, 9,* e51972.
20. Nitzan, N., Swanson, R., Schmitz, D., & Buzsáki, G. (2022). Brain-wide interactions during hippocampal sharp wave ripples. *Proceedings of the National Academy of Sciences, 119*(20), e2200931119.
21. Pedrosa, R., Nazari, M., Mohajerani, M. H., Knöpfel, T., Stella, F., & Battaglia, F. P. (2022). Hippocampal gamma and sharp wave/ripples mediate bidirectional interactions with cortical networks during sleep. *Proceedings of the National Academy of Sciences, 119*(44), e2204959119.
22. David, F., Schmiedt, J. T., Taylor, H. L., Orban, G., Di Giovanni, G., Uebele, V. N., ... & Crunelli, V. (2013). Essential thalamic contribution to slow waves of natural sleep. *Journal of Neuroscience, 33*(50), 19599-19610.
23. Levenstein, D., Buzsáki, G., & Rinzel, J. (2019). NREM sleep in the rodent neocortex and hippocampus reflects excitable dynamics. *Nature communications, 10*(1), 2478.
24. Logothetis, N. K., Eschenko, O., Murayama, Y., Augath, M., Steudel, T., Evrard, H. C., ... & Oeltermann, A. (2012). Hippocampal–cortical interaction during periods of subcortical silence. *Nature, 491*(7425), 547-553.
25. Vann, S. D., Aggleton, J. P., & Maguire, E. A. (2009). What does the retrosplenial cortex do?. *Nature reviews neuroscience, 10*(11), 792-802.
26. Brennan, E. K., Jedrasiak-Cape, I., Kailasa, S., Rice, S. P., Sudhakar, S. K., & Ahmed, O. J. (2021). Thalamus and claustrum control parallel layer 1 circuits in retrosplenial cortex. *Elife, 10,* e62207.
27. Gao, M., Noguchi, A., & Ikegaya, Y. (2021). The subiculum sensitizes retrosplenial cortex layer 2/3 pyramidal neurons. *The Journal of Physiology, 599*(12), 3151-3167.
28. Opalka, A. N., Huang, W. Q., Liu, J., Liang, H., & Wang, D. V. (2020). Hippocampal ripple coordinates retrosplenial inhibitory neurons during slow-wave sleep. *Cell Reports, 30*(2), 432-441.
29. Todorova, R., & Zugaro, M. (2019). Isolated cortical computations during delta waves support memory consolidation. *Science, 366*(6463), 377-381.
30. Ji, D., & Wilson, M. A. (2007). Coordinated memory replay in the visual cortex and hippocampus during sleep. *Nature neuroscience, 10*(1), 100-107.